ELSEVIER

Journal of Power Sources 69 (1997) 113–124

JOURNAL OF POWER SOURCES

The design and construction of high-performance direct methanol fuel cells. 1. Liquid-feed systems

Martin Hogarth [1], Paul Christensen *, Andrew Hamnett, Ashok Shukla [2]

Department of Chemistry, Bedson Building, The University of Newcastle, Newcastle upon Tyne NE1 7RU, UK

Received 15 July 1996; revised 13 February 1997

Abstract

The construction of a liquid-feed direct methanol fuel cell is described in detail for which the fabrication of active electrodes for both the anode and the cathode compartments has been carefully optimised. Electrodes fabricated by deposition of a catalysed carbon/polytetrafluoroethylene paste onto carbon cloth followed by compaction of the two electrodes onto a Nafion® membrane were found initially to give poor results, but by pre-sintering the paste/cloth mix and using a Nafion sol as a flux during the compaction process much better results were obtained. Peak power densities of 0.079 W cm^{-2} were recorded for a 2 M methanol feed at a current density of 300 mA cm^{-2} and an operating temperature of 80 °C. © 1997 Elsevier Science S.A.

Keywords: Fuel cells; Direct methanol fuel cells; Liquid-feed systems; Design

1. Introduction

The direct methanol fuel cell (DMFC) has attracted considerable attention in the last few years since it offers, at least potentially, an alternative and relatively simple power source for transport. Its advantages include high potential efficiency at low loading, simplicity of construction with few moving parts, intrinsically clean fuel conversion and minimal changes to current re-fuelling practice. Attention recently has focused on DMFC cell designs with solid-polymer electrolytes (SPE) such as Nafion®, since such cells offer considerable engineering advantages. However, there remain real problems with the realisation of this type of fuel cell, even in the SPE configuration: with the best current catalysts, the electro-oxidation of methanol is only rapid at temperatures rather above those ideally suited to current solid-polymer electrolyte technology, and water management of these membranes becomes difficult. In addition, there is considerable methanol permeation across the solid-polymer membranes currently used, leading to loss of fuel conversion efficiency, the necessity for more complex engineering on the cathode side, and the development of a mixed potential at the cathode, further lowering the cell voltage. Some of these problems will only be solved with the development of a new generation of solid-polymer materials with properties tailored to the requirements of the DMFC rather than the chlor-alkali industry; however, advances in catalyst design and performance in the last few years have made it sensible to proceed from the testing of half-cells to the design of SPE systems that can act as precursors to fully-sized fuel cells.

In an SPE cell, the polymeric membrane acts as an electronic insulator between the anode and cathode, but it has excellent protonic conduction properties. By using very thin electrolytes of this type, it has become possible to construct electrode assemblies a fraction of a millimetre in thickness. The fuel cell electrodes in such an assembly usually consist of two thin supported catalyst layers which are bonded directly onto the surface of the ion-exchange membrane [1,2]. The membrane electrode assemblies (MEAs) are the heart of the fuel cell system, but a highly optimised electrode will not function to its full potential if it is not operating under very stringent conditions. The fuel cell electrode is, therefore, mounted within a mechanical framework consisting of two electrically conducting field plates (usually made of graphite) in which channels are fabricated. The ridges between the channels are responsible for the electrical contact with the

* Corresponding author: Tel.: +44 (91) 222 67 86; Fax: +44 (91) 222 69 29.

[1] Present address: Johnson Matthey Technology Centre, Blount's Court, Sonning Common, Reading RG4 9NH, UK.

[2] On leave from the Solid State and Structural Chemistry Unit, Indian Institute of Science, Bangalore-560012, India.

PII S0378-7753(97)02580-9

Table 1
Advantages of liquid feed vs. vapour feed for the direct methanol fuel cells

System	Advantages	Disadvantages
Liquid-feed DMFC	Ease of engineering Lower system size and weight Thinner stack (no separate coolant system) Membrane hydration simpler	More dilute methanol reaches anode Methanol is in the form of microbubbles Maximum temperature < 90 °C at practical pressures Lower activities Requires liquid diffusion electrodes
Vapour-feed DMFC	No methanol dilution Higher temperatures of operation resulting in better electrode performance Better response to change of load above 65 °C Can use existing gas diffusion electrodes	Engineering more complexe Larger and heavier system Thermal balance difficult to control Needs cooling system Needs humidification for membrane hydration

backs of the electrodes and conduct the current to an external load, and the channels supply fuel and oxidant respectively to the two sides of the electrode assembly. This MEA, together with a number of subsystems, is capable of sustaining the necessary operating environment for optimum performance.

There are a number of subsystems outside electrode housing:

1. A fuel injection system is required for fuel delivery to the electrode surface. In the case of the DMFC, the fuel mixture can be supplied as a gas or as a liquid.
2. An oxidant system is required, which is responsible for delivering oxygen or air to the electrode surface. For the more unusual applications in which pure oxygen is required, a simple pressurised oxygen tank with a constant pressure regulator would be adequate. However, for most practical, commercial applications, the fuel cell will operate on air as oxidant. There are two distinct approaches: (i) the use of ambient air, or (ii) the use of air at elevated pressures. In principle the use of ambient air as oxidant would be the more desirable from the point of view of system design, since air compressors would constitute a serious parasitic energy drain on the fuel cell in operation. However, as our results below show, cell performance increases as the oxidant pressure is increased, so for a given power rating, cell size decreases as oxidant pressure increases.

The wide range of operating temperatures possible with an SPE fuel cell system means that methanol can be supplied as a vapour or a liquid. From an engineering standpoint, the liquid feed system is the simplest. In such a system, the water acts as a vector for moving methanol into the cell, and also acts as an efficient vector for excess heat removal. Vapour systems, although offering higher performance, have much more difficult start-up problems since fuel pre-heating is necessary before injection. In the case of an SPE cell, where the hydrated perfluorosulfonate ionomer membrane (such as Nafion) is the electrolyte, water control is very important. The conductivity of these membranes generally decreases with decreasing water content [3]. Thus, the maximum attainable amount of water in the membrane is desirable. This is more easily achieved when using a liquid-feed system. The relative advantages and disadvantages of the liquid and vapour-feed systems for the DMFC are outlined in Table 1.

In our work, two single fuel cells, one designed to function with liquid-feed and the other with gaseous feed, have been constructed to a number of strict guidelines. These include:

1. The cell must be constructed from low corrosion-risk materials, particular attention being paid to the operating environment of each cell component. As an example, a high-quality stainless steel may not be attacked by an acidic environment on the bench top, but the situation may well be different if the stainless steel is within a fuel cell held at a positive potential where leaching of one or more components may occur.
2. The cell must be constructed from thermally conducting materials to allow efficient heat transfer to-and-from the electrode assembly.
3. Bulky designs should be avoided, making cells lighter and cheaper to produce.
4. Complex designs requiring time-consuming machining during construction must be avoided.

These principles are illustrated in the designs shown below and in the next paper, and in this first report, we concentrate on liquid-feed systems alone.

2. Experimental

2.1. Cell designs

The liquid-feed system originated with a peristaltic pump, which circulated a liquid methanol/water fuel mixture around the cell; by pre-heating the fuel mixture, cell cooling was minimised. The basic design is shown in Fig. 1: a methanol/water mixture was pumped through a 1 m length of silicone

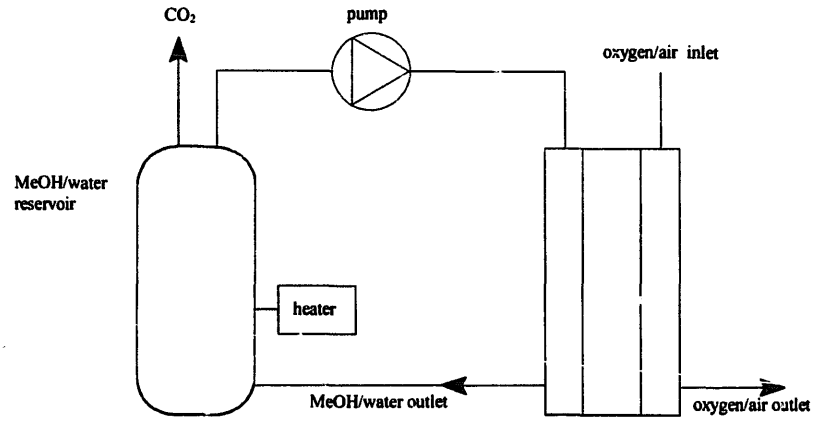

Fig. 1. Block diagram of liquid-feed delivery system.

rubber tubing which was immersed in hot water (60 °C) to pre-heat the fuel mixture before injection into the cell. The peristaltic pump allowed accurate control of the flow rate between the limits 0.046–5 cm^3/min with the possibility of further increasing the flow rate by using additional tubing. The exhaust outlet of the fuel cell was connected to the fuel reservoir with silicone tubing allowing recirculation of any unused methanol.

The oxygen/air used during the DMFC experiments was stored in pressurised cylinders and received no pre-heating or humidifying. The gas supply was regulated, and the flow controlled, with a dedicated fine adjustment needle valve. The gas travelled through a polytetrafluoroethylene (PTFE) tube and was connected to the cell by silicone tubing. The gas pressure was elevated by restricting the passage of the emerging gas from the cell exhaust and taking advantage of the internal gas pressure of the storage cylinder. The flow of gas from the cell was restricted using a simple pressurisation apparatus: the cell exhaust was fitted with a silicone rubber tube which was connected in series with a mercury U-tube. The gas flow was restricted using a tube clamp and the gas pressure was measured by the height of the mercury column. The water produced within the cell was carried into a reservoir by gravity. This pressurisation system was suitable for pressure up to +80 mmHg above ambient (1.1 bar), but above this pressure there was gas leakage, and a separate system was devised for the vapour-feed experiments described in the subsequent paper.

The rigid frame of the cell is the main cell body in which the electrode is housed and includes the field plates, the flow channels and the gasket system which is needed to effect pressurisation of the cell. It was assembled together with compression rods which were tightened under finger pressure with wing-nuts. Each cell contained a recess at the back of each field plate to hold a heating pad of area 26 cm^2 (Watlow 220 V 10 W) and a small hole running parallel with the surface of the plate to hold a thermocouple junction wire (Chromel-Alumel, ice junction).

The cell was constructed mainly with composite plastic materials to the design specification shown in Fig. 2. PTFE–mica composites were used in the construction because they have very low electrical conductivity but high thermal conductivity. Each plate had two bore holes in one of its narrow sides into which hollow stainless-steel screws were fitted. The bore holes emerged at a right angle out through the front face of the block at opposite corners of the electrode. The

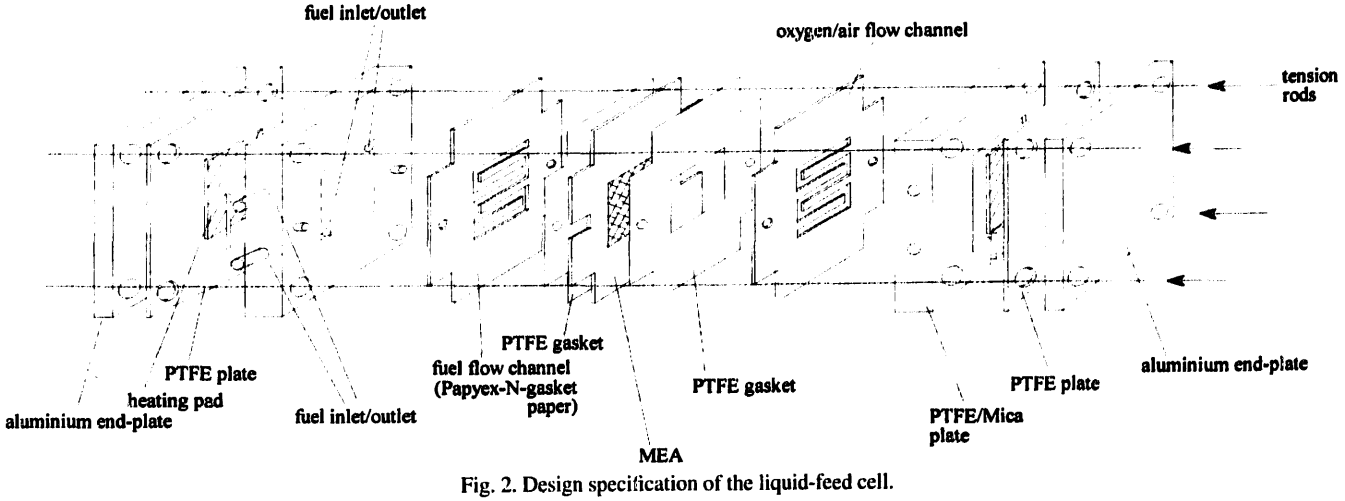

Fig. 2. Design specification of the liquid-feed cell.

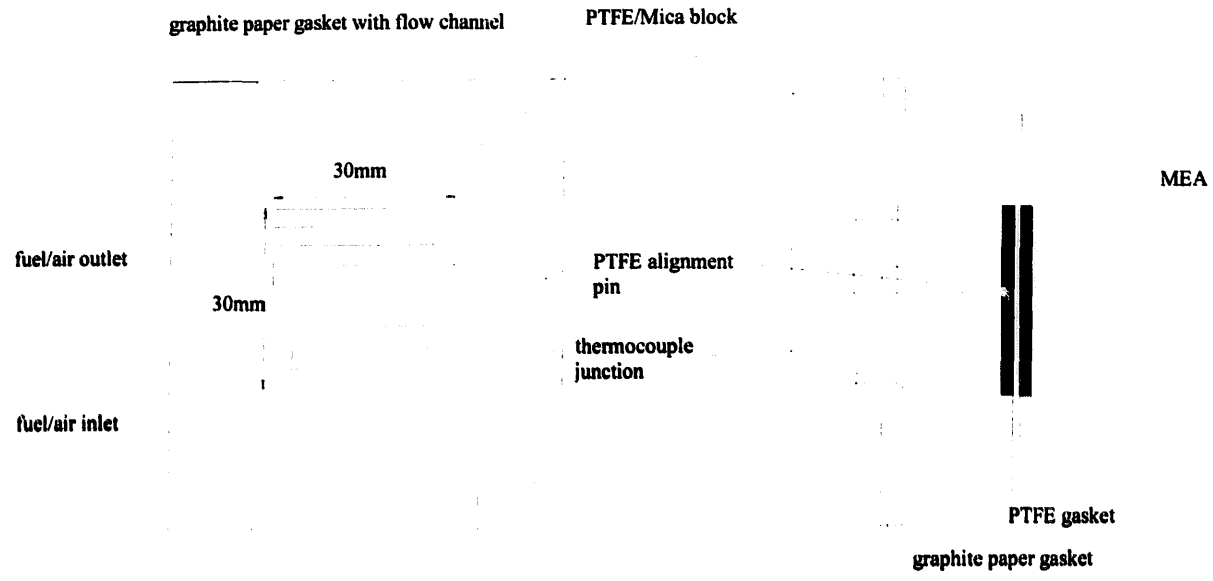

Fig. 3. Flow channel design specification of the liquid-feed cell.

fuel and oxidant injection systems were connected to the hollow steel screws with silicone rubber tubing which was clamped to maintain a seal. One plate was fitted with two PTFE alignment pins which conveniently held the electrode and gaskets in place. The other plate had receiving holes in corresponding positions to accept the alignment pins. Two flow channels of area 9 cm^2 were cut by hand into separate pieces of graphite gasket paper (Le Carbone, Papyex N, 1 mm thick) together with 6 suitable holes to take the compression rods and alignment pins. The flow channels were fitted adjacent to each PTFE–mica block. Fig. 3 illustrates the design of the flow channels and the relative positions of the inlet and outlet holes.

PTFE gaskets (0.1 mm thick) were fitted adjacent to the graphite paper flow channels to act as efficient gas seals around the edge of the Nafion membrane, and presented an electrode area of 6 cm^2. However, the current densities were adjusted to 2 cm^2 which corresponds to the open channel area of the flow pattern. In this manner the Nafion membrane around the carbon layer was protected from direct contact with methanol which would otherwise rapidly permeate through the bare membrane to the cathode. Two integrated heating pads were placed in the recess at the back of the PTFE–mica block and were clamped in place against PTFE sheets (4 mm thick) and an aluminium plate. Finally, two thin brass foils were placed in contact with each graphite paper flow channel to act as current collectors.

The design of the cell was very compact, having a volume of 250 cm^3 with a corresponding weight of 0.65 kg. However, although the cell functioned adequately, a number of problems were encountered with its design and construction. The major components of the cell were constructed using PTFE–mica composite materials and were kept to the minimum possible thickness. During cell operation, the PTFE–mica blocks had a tendency to warp and become mismatched with each other because they were not completely rigid, leading to severe leakage. This problem could only be reversed by clamping the plates against a flat surface and heat-treating them at 200 °C followed by slow cooling, so that a flat surface was restored. There were a number of other sealing problems with the cell as a result of the fact that the majority of connections with the cell and gas-feed systems were made with silicone rubber tubing. This restricted the cells maximum operating pressure to +80 mmHg above ambient (1.1 bar) as indicated above. These problems have subsequently been addressed in a second design described in the next paper in this series, but results for the liquid-feed systems were all obtained with the cell design described above.

2.2. *Electrode fabrication processes*

Three types of electrode fabrication technique were investigated for the liquid-feed cell described above. The first generation of electrode assemblies (Type A1) were developed as an extension of the techniques used for half-cell electrode manufacture [4]; however, these electrodes proved to have rather low performance which necessitated the development of new electrode fabrication techniques, as described below.

Each of the electrodes described below was prepared from Pt–Ru (1:1 atomic ratio) and Pt catalysts at the anode and cathode, respectively. These catalyst materials were prepared from the metal sulfito salts as follows [4–9].

Untreated Ketjen Black EC-600 JD carbon powder was dispersed in Millipore conductivity water at 60 °C. The suspension was placed in an ultrasonic bath for 15 min followed by vigorous mechanical stirring for a further 15 min. The appropriate quantities of the sulfito complexes (Na_6Pt-

Table 2
Electrodes of type A

	Electrode composition		Pressing conditions
	Anode	Cathode	
A1	40wt.%Pt–Ru (3 mg Pt/cm^2) 15 wt.% PTFE 5 wt.% Nafion	15 wt.% Pt (1.6 mg Pt/cm^2) 15 wt.% PTFE 5 wt.% Nafion	200 kg/cm^2 85 °C 10 min
A2	40wt.%Pt–Ru (3 mg Pt/cm^2) 15 wt.% PTFE 5 wt.% Nafion	15 wt.% Pt (1.6 mg Pt/cm^2) 15 wt.% PTFE 5 wt.% Nafion	150 kg/cm^2 135 °C 180 s

$(SO_3)_4$, with $Na_4Ru(SO_3)_3$ for the anode) were dispersed in Millipore conductivity water and the pH was adjusted with 1 M H_2SO_4 to 3 to effect dissolution. This solution was carefully mixed with the carbon suspension and the pH readjusted to 3 if necessary. The carbon suspension was stirred for a further 30 min, an excess of H_2O_2 was added with continuous stirring, after which O_2 and a small quantity of SO_2 were evolved, and the suspension further stirred for 1 h. Following boiling for 5 min the suspension was filtered, and the residue then washed with copious quantities of boiling Millipore conductivity water before drying in air overnight at 110 °C.

2.3. Electrodes of type A

The anode and cathode porous-carbon gas-diffusion layers were both prepared in an identical manner, as follows.

A weighed quantity of catalysed carbon was suspended in a small quantity of Millipore conductivity water and isopropanol (2:1). Appropriate quantities of PTFE suspension and Nafion solution were then added, and the suspension carefully heated at 60 °C with constant mechanical agitation until a putty-like paste was formed. This catalysed carbon paste was evenly spread onto a carbon cloth to a thickness of about 1 mm and of geometric area 9 cm^2. The carbon electrodes were then assembled and aligned on opposite sides of a Nafion membrane (10 cm × 10 cm) and placed between two stainless-steel plates with a non-stick paper backing (Easy Bake™ siliconised parchment). The complete electrode assembly was placed into a hydraulic press and gradually heated over a 5 min period to the appropriate pressing temperature under a load of 1 kg, following which the electrode was compacted. After compaction, the electrode assembly was submerged in cold Millipore conductivity water for 2 h to re-hydrate the membrane, and then mounted into the fuel cell. Table 2 summarises the composition and the compaction conditions used during fabrication of the MEAs with this fabrication protocol. The anode layer consisted of a 40wt.%Pt–Ru catalyst with the Pt loading fixed at 3 mg cm^{-2}, and the cathode layer a 15 wt.% Pt catalyst with the Pt loading fixed at 1.6 mg cm^{-2}.

2.4. Electrodes of type B

An alternative electrode fabrication technique was devised, in which the electrode surface was brush-coated with Nafion solution before compaction. In this manner, the electrode surface contained a higher concentration of Nafion than the bulk of the electrode to aid bonding between the electrodes and the membrane.

Table 3 summarises the composition and the compaction conditions used during fabrication of MEAs with this protocol. The anode consisted of a 40wt.%Pt–Ru catalyst with the Pt loading maintained at 3 mg cm^{-2}, and the cathode a 10 wt.% Pt catalyst with the Pt loading maintained at 1.1 mg cm^{-2}. Each electrode contained a 20 wt.% PTFE loading and a Nafion loading of 1 mg cm^{-2}. Both the anode and the cathode porous carbon electrodes were prepared in an identical manner as described below.

The catalysed carbon/PTFE paste, prepared as for Type A electrodes but without Nafion solution, was evenly spread onto a carbon cloth to a thickness of about 1 mm and of geometric area 9 cm^2. These carbon electrodes were immediately painted with Nafion solution to give a loading of 1 mg cm^{-2}. The electrodes were dried in air for 30 min before heating at 110 °C under vacuum for 1 h.

After drying, the electrodes were hydrated by soaking for 30 min in hot Millipore conductivity water. The softened electrodes were then assembled with a pre-treated Nafion membrane and placed between two stainless-steel plates with a non-stick paper backing. The complete electrode assembly was then gradually heated over a 5 min period to the pressing temperature under a load of 1 kg. Electrode assemblies were compacted employing the conditions outlined in Table 3. A variety of compaction pressures and times were used and each electrode was compacted at 130 °C. Following compaction, the electrode assemblies were submerged in cold Millipore conductivity water for 2 h to allow membrane hydration, and were then mounted into the cell.

2.5. Electrodes of type C

Electrodes of Type B were found to be quite superior to those of Type A but were nevertheless susceptible to crack-

Table 3
Electrodes of type B

	Electrode composition		Pressing conditions
	Anode	Cathode	
B1	40wt.%Pt–Ru (3 mg Pt/cm^2) 20 wt.% PTFE 1 mg Nafion/cm^2	10 wt.% Pt (1.1 mg Pt/cm^2) 20 wt.% PTFE 1 mg Nafion/cm^2	50 kg/cm^2 135 °C 180 s
B2	40wt.%Pt–Ru (3 mg Pt/cm^2) 20 wt.% PTFE 1 mg Nafion/cm^2	10 wt.% Pt (1.1 mg Pt/cm^2) 20 wt.% PTFE 1 mg Nafion/cm^2	150 kg/cm^2 135 °C 90 s
B3	40wt.%Pt–Ru (3 mg Pt/cm^2) 20 wt.% PTFE 1 mg Nafion/cm^2	10 wt.% Pt (1.1 mg Pt/cm^2) 20 wt.% PTFE 1 mg Nafion/cm^2	150 kg/cm^2 135 °C 180 s
B4	40wt.%Pt–Ru (3 mg Pt/cm^2) 20 wt.% PTFE 1 mg Nafion/cm^2	10 wt.% Pt (1.1 mg Pt/cm^2) 20 wt.% PTFE 1 mg Nafion/cm^2	300 kg/cm^2 135 °C 90 s
B5	40wt.%Pt–Ru (3 mg Pt/cm^2) 20 wt.% PTFE 1 mg Nafion/cm^2	10 wt.% Pt (1.1 mg Pt/cm^2) 20 wt.% PTFE 1 mg Nafion/cm^2	300 kg/cm^2 135 °C 180 s
B6	40wt.%Pt–Ru (3 mg Pt/cm^2) 20 wt.% PTFE 1 mg Nafion/cm^2	10 wt.% Pt (1.1 mg Pt/cm^2) 20 wt.% PTFE 1 mg Nafion/cm^2	400 kg/cm^2 135 °C 90 s
B7	40wt.%Pt–Ru (3 mg Pt/cm^2) 20 wt.% PTFE 1 mg Nafion/cm^2	10 wt.% Pt (1.1 mg Pt/cm^2) 20 wt.% PTFE 1 mg Nafion/cm^2	400 kg/cm^2 135 °C 180 s

Table 4
Electrode type C1

	Electrode composition		Pressing conditions
	Anode	Cathode	
C1 [a]	40wt.%Pt–Ru (3 mg Pt/cm^2) 20 wt.% PTFE 1 mg Nafion/cm^2	10 wt.% Pt (1.1 mg Pt/cm^2) 20 wt.% PTFE 1 mg Nafion/cm^2	150 kg/cm^2 135 °C 180 s

[a] Anode and cathode compacted under 200 kg/cm^2 for 10 min prior to sintering.

ing. This problem was eliminated by modifying the electrode fabrication technique by including a sintering process similar to the one used during half-cell manufacture [4].

Anodes were prepared from a 40wt.%Pt–Ru catalyst with the Pt loading fixed at 3 mg cm^{-2}, and the cathodes prepared from a 10 wt.% Pt catalyst with the Pt loading fixed at 1.1 mg cm^{-2}. Each electrode contained a 20 wt.% PTFE loading and a 1 mg cm^{-2} Nafion loading. The electrodes were prepared as follows.

The catalysed carbon/PTFE paste, prepared as for Type B electrodes, was evenly spread onto a carbon cloth to a thickness of about 1 mm and geometric area 9 cm^2. The electrodes were then cold pressed for 10 min using a pressure of 200 kg cm^{-2} followed by sintering in air at 350 °C for 30 min, after which they were brush coated with Nafion solution to give the required loading and allowed to dry in air for 10 min. The electrodes were assembled with a Nafion membrane and placed between two stainless-steel plates with a non-stick paper backing. The complete electrode assembly was gradually heated over a 5 min period to the pressing temperature under a load of 1 kg and compacted employing the conditions outlined in Table 4. Following compaction, the electrode assemblies were immediately soaked in cold Millipore conductivity water for 2 h prior to mounting in the cell.

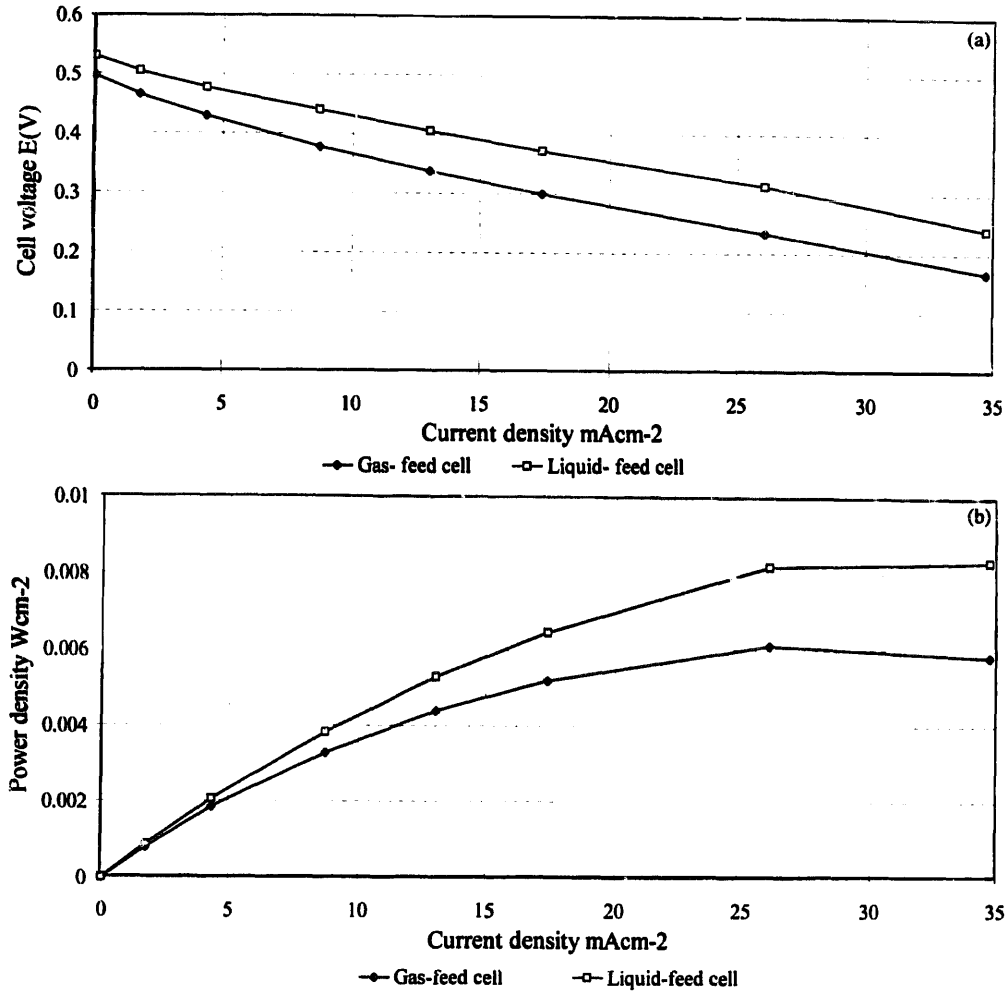

Fig. 4. (a) Polarisation curves for electrode A1 tested with carrier-gas and liquid-feed at 70 °C using 2.5 M methanol and ambient oxygen. (b) Power density of electrode A1 tested with carrier-gas and liquid-feed at 70 °C using 2.5 M aqueous methanol and ambient oxygen.

None of the results given in this paper have been corrected for *iR* loss.

3. Results and discussion

3.1. Electrodes of type A

The electrodes were mounted in to the cell described above, which was coupled in-turn with the liquid-feed and pressure systems previously described. The fuel and oxidant feeds were engaged and the MEA conditioned for 1 h without current loading with ambient oxygen pressure. Galvanostatic polarisation data for electrode A1 at 70 °C is shown in Fig. 4(a).

An open-circuit potential (OCV) of 0.53 V was recorded for the cell, representing a considerable rest overpotential [10–12]. At a current loading of 25 mA cm^{-2}, the cell voltage was 0.32 V, and Fig. 4(b) shows the electrode power density as a function of current density. For comparison, some vapour-feed data for methanol carried in with N_2 carrier gas is also presented for this cell, showing that for this electrode configuration, liquid-feed is rather better.

A peak power density of 0.008 W cm^{-2} was obtained for the liquid-feed cell with this configuration, a very disappointing result, requiring a 25-fold improvement to reach the target power density of 0.2 W cm^{-2} which is believed to be essential for transport applications. The galvanostatic data for electrode A1 had a slope (area resistance) of 7.6 Ω cm^2 which is extremely high compared with the values usually quoted for optimised H_2/O_2 electrodes which typically have area resistances of about 0.2 Ω cm^2 [13,14], indicating substantial ohmic losses across our electrode.

The performance of the A1-type electrode was disappointing in view of the success with similarly fabricated half-cell electrodes [4]. However, the data obtained from the half-cells employed liquid sulfuric acid electrolyte, for which a high ionic conductivity would be maintained throughout the whole electrode, even if there was poor contact with the polymer electrolyte membrane. The origin of the high ohmic

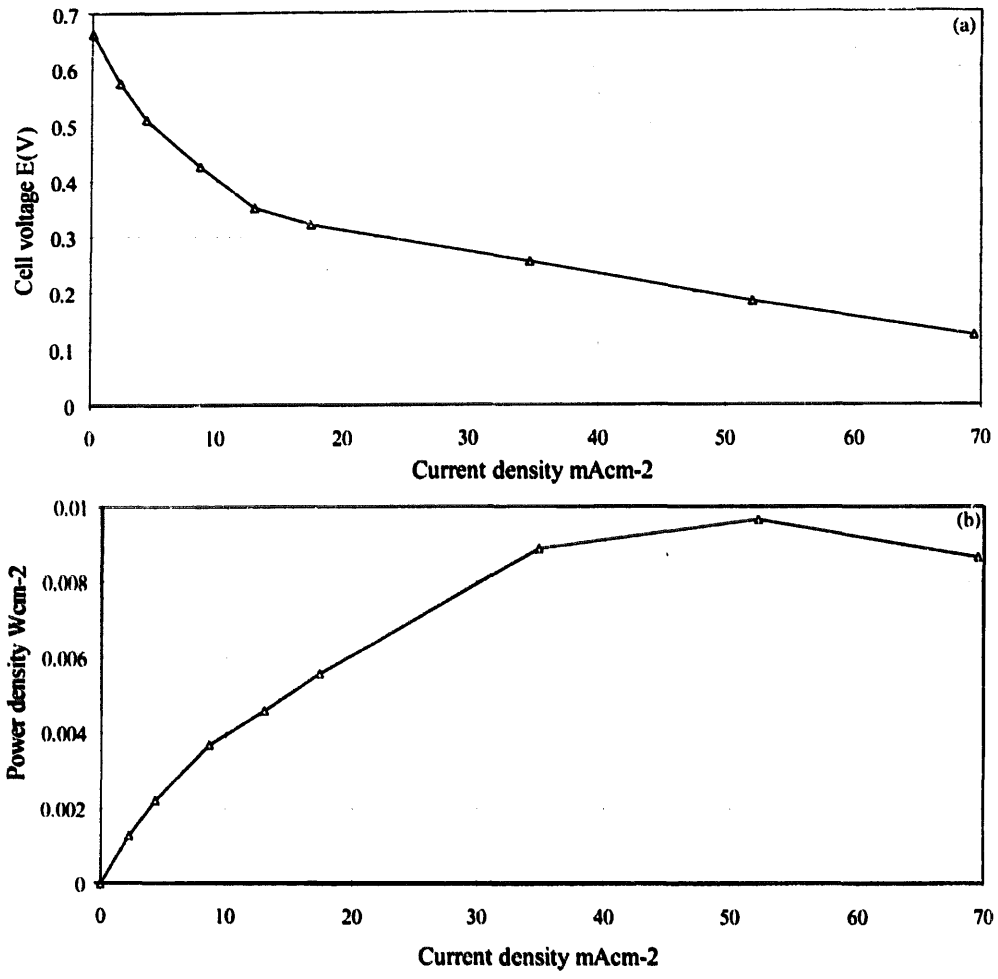

Fig. 5. (a) Polarisation curve for electrode A2 with liquid-feed at 70 °C using 2.5 M aqueous methanol and ambient oxygen. (b) Power density of electrode A2 with liquid-feed at 70 °C using 2.5 M aqueous methanol and ambient oxygen.

losses was revealed by scanning electron microscopy (SEM) examination of electrode cross sections which showed that the anode layer did not appear to be effectively bonded to the Nafion membrane as was the case of the cathode layer. For some electrodes, this caused complete de-lamination of the anode layer from the electrode assembly. Since the anode/cathode electrode compositions were identical but for the catalyst loading, the lack of adhesion between anode and SPE was presumably a wetting problem caused by the hydrophobic catalyst layer.

Fig. 5(a) and (b) shows the performance of Type A2 electrodes operating under identical conditions. A small improvement in performance was seen by increasing the compaction temperature towards the softening point of the Nafion membrane; this probably improved the interfacial contact between the Nafion membrane and the porous carbon electrodes. The area resistance of electrode A2 was significantly reduced to a value of about 3.6 $\Omega\,cm^2$ which was considerably lower than that of electrode A1, but at best the power density only approached 0.01 W cm^{-2}. The low activities attained by Type A electrodes suggests the lack of an efficient gas diffusion structure both as a mediator of reactants to the catalyst surface, and as a rapid pathway for proton migration through the electrode, and an improvement was sought.

3.2. Electrodes of type B

Fig. 6(a) and (b) shows the performances of electrodes B1–B7 at 76 °C. Prior to testing, each electrode was conditioned for 2 h after mounting in the cell by admitting a constant supply of 2.5 M aqueous methanol to the anode and ambient oxygen to the cathode. Steady-state galvanostatic polarisation data were recorded for a range of current densities using 2.5 M methanol solution pumped at a flow rate of 0.23 cm^3/min, and ambient oxygen. Electrodes were tested a number of times until a steady performance was reached, typically after five polarisation experiments.

A comparison of the cell voltages at 100 and 200 mA cm^{-2}, and the peak power densities are given in Table 5.

The performance of each Type B electrode was approximately three to five times higher than that of the Type A electrodes. The poorest performance was attained by elec-

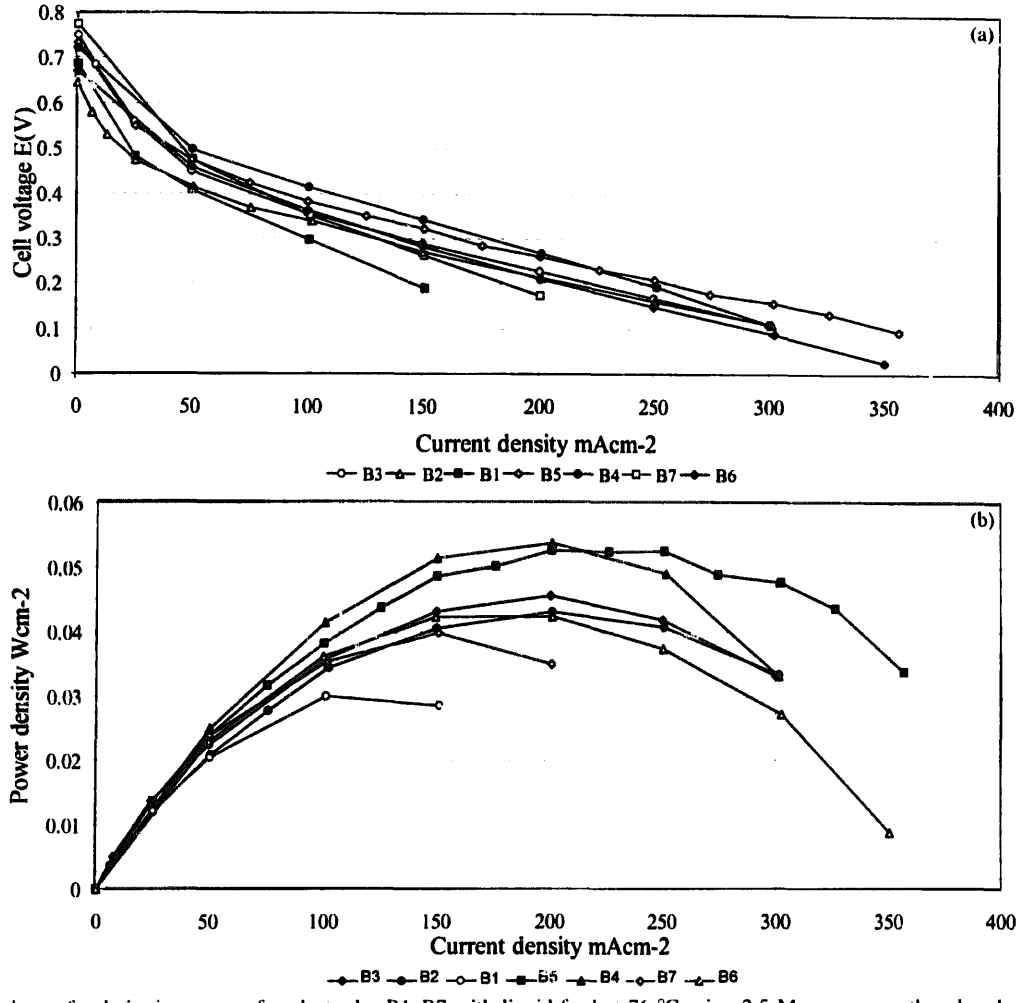

Fig. 6. (a) Comparison of polarisation curves for electrodes B1–B7 with liquid-feed at 76 °C using 2.5 M aqueous methanol and ambient oxygen. (b) Comparison of electrode power densities for electrodes B1–B7 with liquid-feed at 76 °C using 2.5 M aqueous methanol and ambient oxygen.

trode B1 which gave a cell voltage of 0.3 V at 100 mA cm^{-2} and a peak power density of 0.03 W cm^{-2}; however, after compaction electrode B1 partially de-laminated during soaking, and undoubtedly the poor performance was related to this. The highest cell performance came from electrode B5, which was compacted at a higher pressure of 300 kg cm^{-2} for 180 s. This electrode gave a voltage of 0.38 V at 100 mA cm^{-2} and 0.27 V at 200 mA cm^{-2}, with a peak power output of 0.053 W cm^{-2}. However, the performance of the subsequent electrode, compacted at higher pressures, was reduced. This was probably a result of the electrode structure being crushed or distorted at the higher compaction pressure, which significantly reduced the accessibility of the reactants, particularly at higher current densities.

Table 5
Comparison of the cell voltages at 00 and 200 mA/cm^2, and the peak power densities, for electrodes B1–B7

Electrode	Cell voltage E (V)		Peak power density W/cm^2
	100 mA/cm^2	200 mA/cm^2	
B1	0.3		0.03
B2	0.34	0.22	0.043
B3	0.37	0.23	0.046
B4	0.41	0.28	0.054
B5	0.38	0.27	0.053
B6	0.37	0.21	0.04
B7	0.34	0.18	0.043

Electrode B7 had an area resistance of about 1 Ω cm^2 which was a considerable improvement on the previous electrode type. Examination of the electrode cross sections with SEM showed good contact between the electrodes and the membrane, but the electrodes were susceptible to cracking during the fabrication process, and these cracks are particularly prominent in the cathode layer, undoubtedly contributing significantly to the ohmic losses.

Fig. 7(a) and (b) shows the effect of pressurising electrode B7 at an oxygen pressure of 1.05 bar. In addition, the effect of increasing the methanol concentration is also shown for the same electrode. The effect of cathode pressurisation was small at lower current densities: the cell voltages were

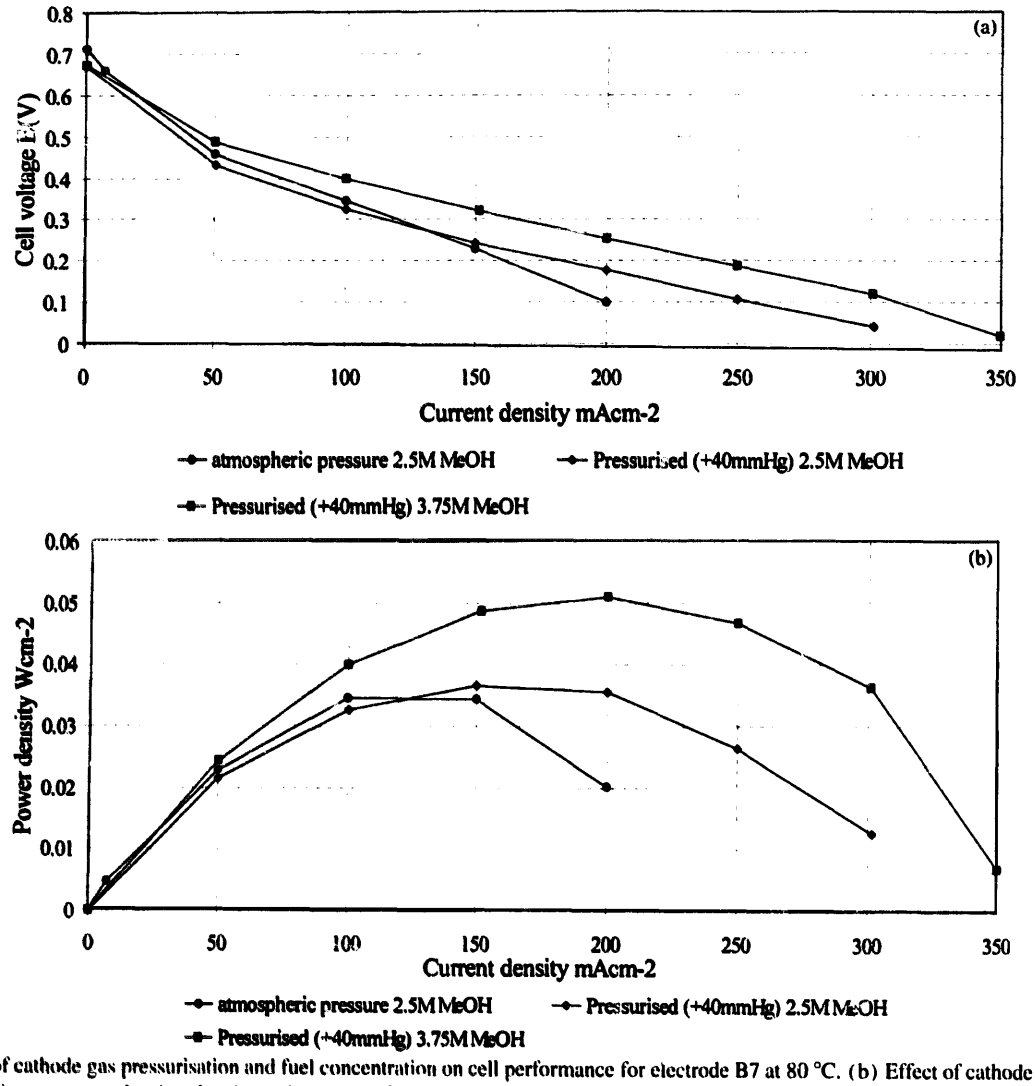

Fig. 7. (a) Effect of cathode gas pressurisation and fuel concentration on cell performance for electrode B7 at 80 °C. (b) Effect of cathode gas pressurisation and fuel concentration on power densisty for electrode B7 at 80 °C.

0.34 and 0.32 V at 100 mA cm^{-2} with and without pressurisation, respectively. At higher oxygen pressures, the cell was more able to sustain higher current densities. The peak power densities of the two cells were quite similar, with the unpressurised cell producing 0.035 W cm^{-2} at 100 mA cm^{-2}, and the pressurised cell 0.037 W cm^{-2} at 150 mA cm^{-2}.

It can be seen from Fig. 7(a) that the type B electrodes show a marked improvement in OCV compared with those of type A, of about 200 mV.

Increasing the methanol concentration to 3.75 M with the higher oxygen pressure resulted in a large increase in the cell performance. The cell voltage increased to 0.4 V at 100 mA cm^{-2} and 0.26 V at 200 mA cm^{-2} with a peak power density of 0.051 W cm^{-2}. This suggested that mass transport limitations were also in effect at the anode, which were somewhat reduced with higher methanol concentrations. However, it should be stressed that subsequent increases in the methanol concentration led to significant decreases in the cell voltage presumably as a result of methanol permeation to the cathode.

It is clear that improved interfacial bonding between the porous carbon electrodes and the Nafion membrane has led to substantial reductions in the ohmic losses, and hence increase in electrode performances. The peak power density for electrode B5, when operating with liquid 2.5 M methanol and ambient oxygen, was 0.053 W cm^{-2} at 200 mA cm^{-2} which was considerably higher than that attained by the previous electrode type. Unfortunately, the porous carbon electrodes were found to crack severely during the fabrication process, decreasing the efficacy of the gas diffusion structure, and contributing to ohmic losses.

3.3. Electrodes of type C

Fig. 8(a) and (b) shows the performance of electrode C1 mounted into the cell at 80 °C operating with a variety of methanol concentrations, and an oxygen pressure of 1.1 bar.

Again, the type C1 electrode showed an OCV of about 0.70–0.75 V, comparable with the best of the B electrodes,

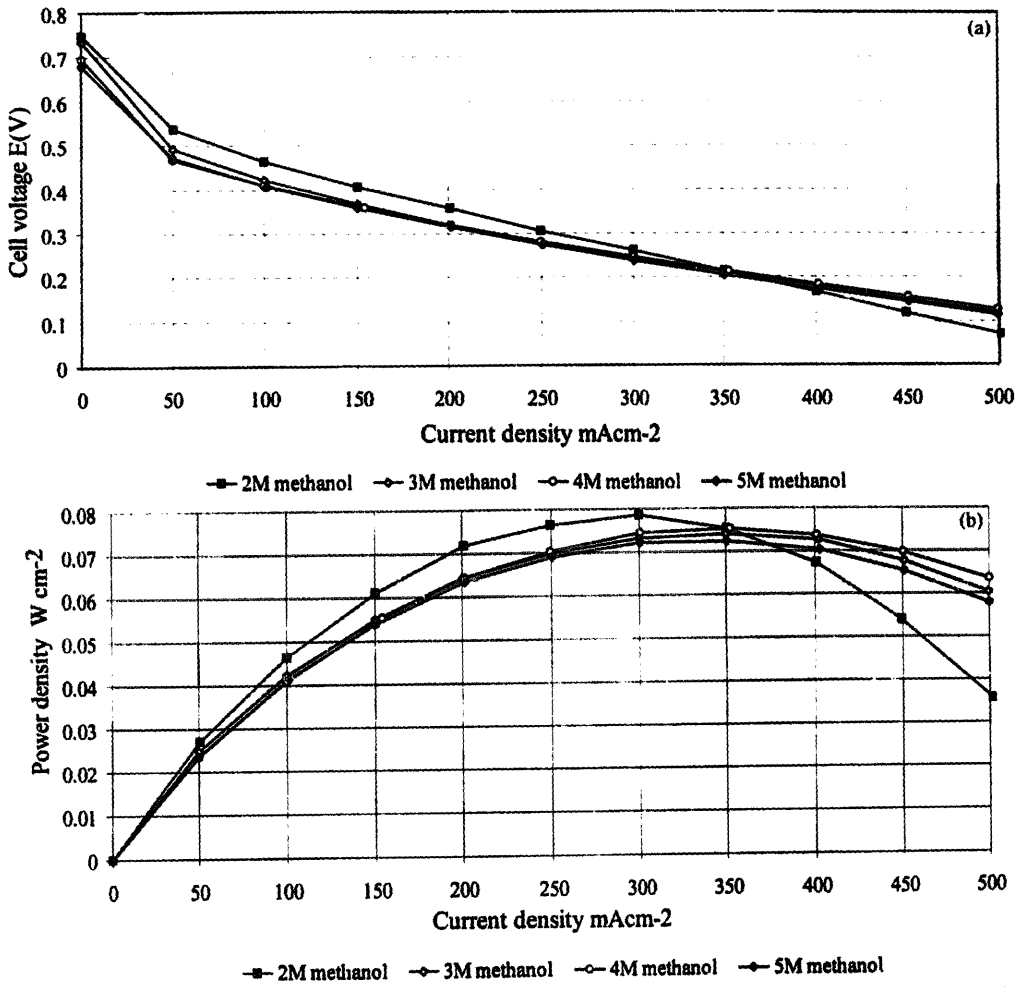

Fig. 8. (a) Effect of methanol concentration on the cell voltage for electrode C1 at 80 °C using pressurised oxygen (1.1 bar). (b) Effect of methanol concentration on power denisty for electrode C1 at 80 °C using pressurised oxygen (1.1 bar).

and significantly better than the type A electrodes. Given that the catalyst is essentially the same for both MEAs, this improvement suggests that the low OCV found for the A electrodes may reflect significantly higher permeation rates for methanol.

Lower methanol concentrations (2 M) were favoured at current densities below 350 mA cm^{-2}, with cell voltages of 0.47 and 0.36 V at 100 and 200 mA cm^{-2}, respectively. A peak power density of 0.079 W cm^{-2} was recorded for 2 M methanol at a current density of 300 mA cm^{-2}. For higher methanol concentrations (3.75 M), the peak power density was reduced to ~0.075 W cm^{-2} at a current density of 350 mA cm^{-2}. For 0.5 M methanol, slightly higher performances were obtained at 100 and 200 mA cm^{-2}, but above 300 mA cm^{-2}, there was significant concentration polarisation.

Examination of electrode cross sections verified that the catalyst layers appear to be effectively adhered to the membrane and no cracks were apparent anywhere in the structure. The thickness of the catalyst layer had also been significantly reduced from about 300 μm (Type B) to 200 μm (Type C). Each of these factors contributed to a reduction in the ohmic drop, which is reflected in the area resistance of 0.75 Ω cm^2.

4. Conclusions

It is evident that by attention to the conditions of manufacture of MEAs, quite substantial improvements in overall performance can be attained. The structure of the carbon electrodes was improved by pre-compacting the electrodes, followed by a sintering process. This has eliminated the severe electrode cracking that was a problem with the dry-electrode fabrication process. The catalyst layers have also been reduced to a thickness of about 200 μm which has reduced the ohmic losses. Performances of close to 0.1 W cm^{-2} are extremely encouraging for liquid-feed systems, though it is clear that further improvements in electrode design are possible, and these have been particularly effective for vapour-feed systems as described in the next paper.

Acknowledgements

We gratefully acknowledge the Royal Society for a Visiting Fellowship to A.S., and the EPSRC for a studentship (to M.P.H.) and a post-doctoral fellowship (to A.S.). We are also grateful to the EU for funding under the Joule II project. We also acknowledge the enormous help given to us by Mr Roland Graham and Mr Alan Knox of the Chemistry mechanical workshops. Finally, we thank Professor K. Scott for helpful discussions.

References

[1] H.P. Dhar, *J. Electroanal. Chem.*, *357* (1993) 237–250.
[2] O.L. Murphy, G.D. Hitchens and D.J. Manko, *J. Power Sources*, *47* (1994) 353–368.
[3] T.A. Zawodzinski, T.E. Springer, J. Davey, J. Valero and S. Gottesfeld, *Proc. Symp. on Modelling of Batteries and Fuel Cells*, The Electrochemical Society, Vol. 93-10, Pennington, NJ, USA, 1993.
[4] M.P. Hogarth, P.A. Christensen and A. Hamnet, *Proc. 1st Int. Symp. Fuel Cell Systems, Montreal, Canada, 1995*, pp. 310–325.
[5] M. Watanabe, M. Uchida and S. Motoo, *J. Electroanal. Chem.*, *229* (1987) 395
[6] P. Stonehart, *Ber. Bunsenges. Phys. Chem.*, *94* (1990) 913–921.
[7] H.G. Petrow and R.J. Allen, *US Patent No. 3 992 331* (16 Nov. 1976).
[8] H.G. Petrow and R.J. Allen, *US Patent No. 3 992 512* (16 Nov. 1976).
[9] H.G. Petrow and R.J. Allen, *US Patent No. 4 044 193* (23 Aug. 1977).
[10] EU Contractors Meeting, *Proj. JOUE2-CT92-0102*, Siemens GmbH., June 1994.
[11] S. Surampudi, S.R. Narayanan, E. Varmos, H. Frank, G. Halpert, A. LaConti, K. Kosek, G.K. Surja Prakesh and G.A. Olah, *J. Power Sources*, *47* (1994) 337–385.
[12] ARPA, unpublished data.
[13] O.L. Murphy, G.D. Hitchens and D.J. Manko, *J. Power Sources*, *47* (1994) 353–368.
[14] K. Prater, *J. Power Sources*, *29* (1990) 239–250.